DESIGN OF A BLOOD SERUM ACOUSTIC BIOSENSOR FOR INFERRING PROSTATE CANCER RECURRENCE

Undergraduate Thesis

Presented to
The Academic Faculty
By
Christopher K. Giardina

School of Biomedical Engineering

Georgia Institute of Technology
Atlanta, GA 30332

April 21, 2011

DESIGN OF A BLOOD SERUM ACOUSTIC BIOSENSOR FOR INFERRING PROSTATE CANCER RECURRENCE

To be approved by:

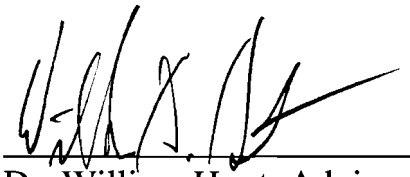

Dr. William Hunt, Advisor
School of Electrical and Computer Engineering
Georgia Institute of Technology

Dr. Carlos Moreno
Department of Pathology and Laboratory Medicine
Emory University

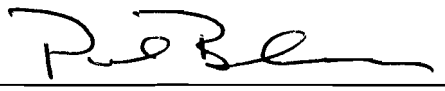

Dr. Paul Benkeser, Associate Chair of Undergraduate Research
School of Biomedical Engineering
Georgia Institute of Technology

TABLE OF CONTENTS

LIST OF ABBREVIATIONS

ALP	Alkaline Phosphatase
BAW	Bulk Acoustic Wave
FBAR	Film Bulk Acoustic Resonator
FITC	Fluorescein Isothiocyanate
PSA	Prostate - Specific Antigen
QCM	Quartz Crystal Microbalance
QCM-D	Quartz Crystal Microbalance with Dissipation
SAM	Self-Assembled Monolayer (alkane thiol with antibodies)
SAW	Surface Acoustic Wave
SIM2	Simple - Minded Homolog 2
ZnO	Zinc Oxide

LIST OF FIGURES

ABSTRACT

Biomarkers and the methods which are utilized to detect them are at the forefront of disease prevention, detection, and prognosis. To further the prostate cancer clinical detection modalities, quartz crystal microbalances with dissipation (QCM-D) were inoculated with a functional layer of antibodies to afford an immuno-specific biosensor capable of reporting frequency, dissipation, and viscoelasticity shifts indicative of changes in surface chemistry. Because serum protein binding occurs selectively at the antibody's paratope and non-selectively at the QCM-D surface, multiple sensors were used simultaneously to isolate the frequency and dissipation shifts due exclusively to the antigen-antibody binding event. Early studies with fluorescein isothiocyanate (FITC) indicated that binding to its respective antibody yielded significantly positive frequency shifts in a dose-dependent fashion, contrary to the Sauerbrey model. The data, however, fits a time-dependent perturbation theory in which surface frequency changes during adsorption are due to both mass and stiffness changes. FITC was further used as a reference sensor to account for the non-specific binding of Bovine Serum Albumin (BSA) in a recombinant BSA solution and several solutions of fetal bovine serum (FBS). FBS was diluted to the same BSA concentration as a recombinant solution and experimentation showed no significant difference in detected frequency shift, despite a large difference in viscosity. These findings indicate that only recombinant protein is necessary when creating dose-response curves for calibrating an assay from this technique. Pure samples of FBS were also studied, and exhibited frequency shifts similar to a multiple of the prior FBS dilution factor. These proof of concept studies allowed for the simultaneous detection of PSA, alkaline phosphatase, and Simple-minded homolog 2 (SIM2) in human serum from patients with either recurrent or non-recurrent prostate cancer. Repeated trials will allow for robust comparison between cohorts.

BACKGROUND

1. Prostate Cancer Biomarker Upregulation

1.1 Prostate Carcinoma

One man in six will be diagnosed with prostate cancer at some time in his lifetime. In 2009, prostate cancer was the most highly diagnosed male cancer, and was the leading cause of cancer-induced deaths after lung cancer. The American Cancer Society also predicts that 217,730 new cases of prostate cancer will be diagnosed and 32,050 patients will die in the 2010 year alone.[1] After radiation and chemotherapy, the risk of prostate cancer recurrence is always present. Currently, no such assay or standardized test exists which assesses the risk of recurrence.

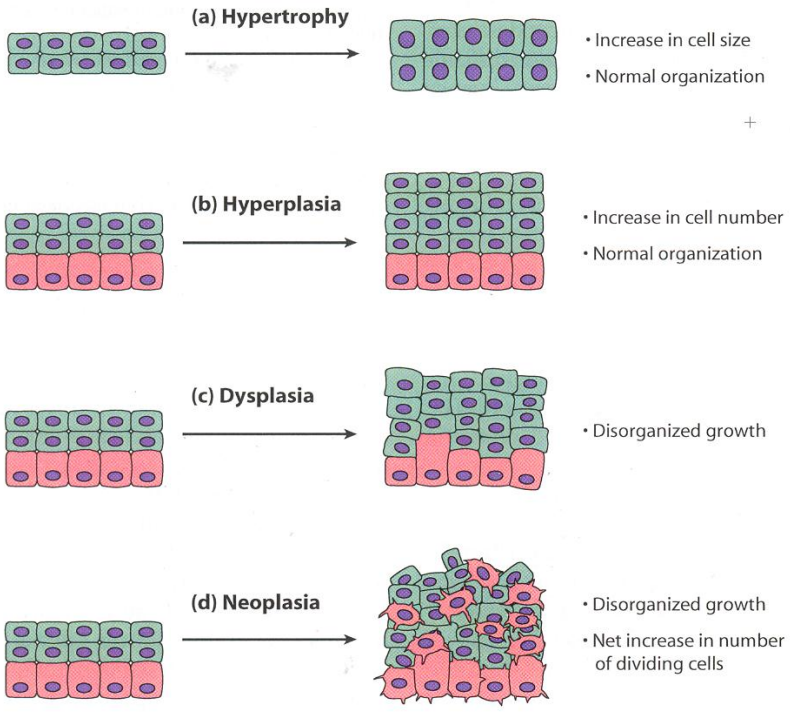

Figure 1: Prostate Cancer Cell Morphologies. As prostate cancer cells progress from benign to malignant, they increase in size (hypertrophy), increase in number (hyperplasia), become disorganized (dysplasia), and grow uncontrollably (neoplasia). Modified.[2]

Although there are several tissue layers within the prostate, 99% of all prostate cancers are adenocarcinomas, arising from the glandular cells which secrete seminal fluid.[2] Cells exhibit cancerous behavior when they acquire traits and defects in regulatory signaling pathways which ultimately augment cell homeostasis. These traits include self-sufficiency in growth signals, insensitivity to antigrowth signals, apoptosis-evading mechanisms, limitless reproductive potential, sustained angiogenesis, and tissue invasion and metastatic mechanisms.[3] As these prostate glandular cells divide uncontrollably, the tissue layers undergo several morphological changes (Figure 1).

1.2 Prostate Cancer Biomarkers and Recurrence

The prostate's high level of interaction with systemic biological queues makes it a prime candidate for determining the stage of the cancer from a blood sample. Protein secretion and expression patterns are drastically different at different stages in the disease and are proposed to vary before and after radiation or chemotherapy (Figure 2).

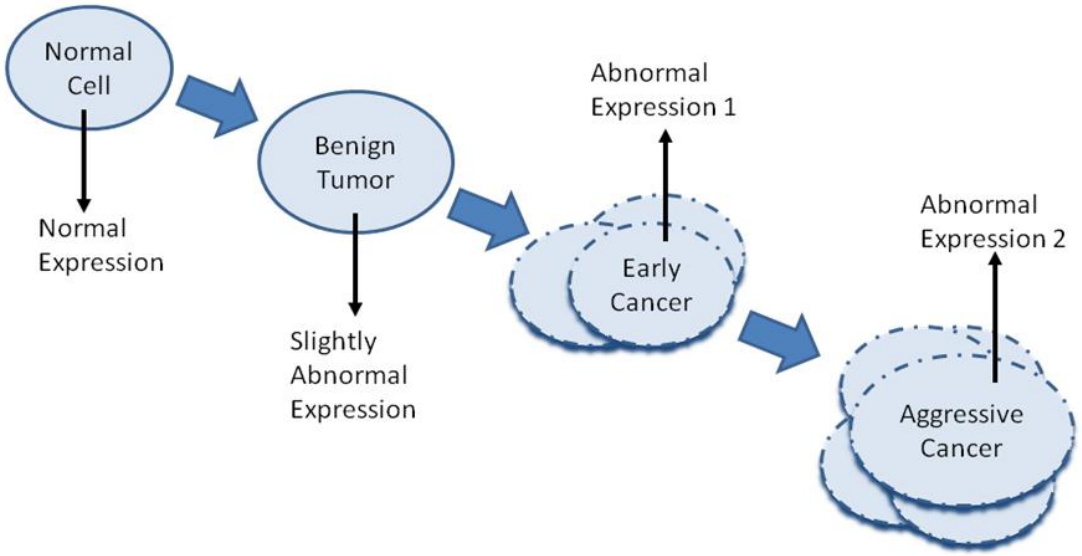

Figure 2: Biomarker Secretion Patterns. As prostate cancer cells progress from benign to malignant to aggressive, their behaviors and secretion patterns differ. However, little research has been conducted to infer recurrence.

With reference to prostate cancer, many markers have been shown to be elevated in human samples (Figure 3). PSA[4], pPSA[5], EPCA-2[6], IGFBP-2[7], APoA-II[8], ZAG[9], T-ALP[10], PICP[10], BAP[10], α CTX[10], β CTX[10], CTX[10], DSPP[11], BSP[11], and OPN[11] have all shown to have increased levels in either serum, urine, or tissue biopsy in human samples. In particular, Prostate-Specific Antigen (PSA) is the gold standard and the only approved serum biomarker that the American Cancer Society endorses for mass screening of the public.[12]

Marker	Molecule Type	Sampled from	Up/Down-Regulated	Notes	Reference
PSA	glycoprotein	serum	+	Gold Standard	4
pPSA (truncated)	glycoprotein (precursor of PSA)	serum	+	More specific than PSA; detects before PSA levels rise	5
EPCA-2	protein	serum	+	Extremely Specific; differentiated between +/- metastatic PCa	6
IGFBP-2	protein	serum	+	Elevation related to tumor stage and PSA	7
ApoA-II	apolipoprotein	serum	+	Detects PC even when PSA levels are low, elevated in benign hyperplasia and PCA	8
ZAG	glycoprotein	serum	+	Also correlated to cachexia, or reduction of vitality and strength	9
T-ALP PICP BAP	protein	tissue biopsy	+	Only compared marker elevations during bone metastasis; cannot differentiate between healthy, indolent, or non-metastatic.	10
α CTX β CTX	telopeptides of Collagen I	urine	+		
CTX	telopeptides of Collagen I	serum	+		
DSPP BSP OPN	integrin-binding proteins	serum	+	DSPP strongest candidate, BSP and OPN don't rise until late in disease	11

Figure 3: Extracellular Serum Biomarkers. Biomarkers in this list have been shown to be significantly elevated when compared to non-cancerous equivalents.

The markers listed inFigure 3 exemplify several of the few markers tested on actual human samples. As tumor tissue becomes increasingly neoplasic, cell disorganization causes a vast number of the cells to lyse due to abnormal stress and strain on the plasma membrane of the cells.[2] The tumor continues to grow in volume, the cells which rupture, and the entire cytosolic contents spill into the surrounding extracellular space.[13] Although these chemicals are usually destroyed via serum proteases, macrophage activity, and renal clearance, increased vasculature due to abnormal angiogenesis permits these highly concentrated intracellular proteins to have increased exposure to systemic circulation. Some protein[14] and DNA[15] levels have been significantly differentiated in cancerous vs. non-cancerous serum.

A Banyard et al. study reviews growth factors, cytokines, hormones, membrane receptors, proteases, actin-binding proteins, tumor-supressor genes, and intracellular signaling proteins which are either up- or down-regulated in human PC3, LNCaP and ARCaP prostate cancer cell lines in terms of both cell motility and metastasis.[16] One study by Varambally et al. attempted to quantify both intracellular and extracellular proteins by analyzing tissue extracts from prostate organs at the time of radical prostatectomy.[14] Although the literature presented in Figure 3 present an "all or nothing" approach to detecting prostate cancer, the Varambally et al. study detected clinically localized benign cancer (Figure 4) and metastatic cancer (Figure 5). There may even be differences after prostate cancer radiation and chemotherapy.

Marker	Molecule Type	Sampled from	Up/Down-Regulated	Notes	Reference
Myosin VI	Protein	Biopsy	+	Verified in 8/9 studies	14
BUB3	Protein	Biopsy	+	Verified in 6/9 studies	
PSA	Protein	Biopsy	+	Verified in 5/9 studies	
Aurora Kinase A	Protein	Biopsy	+	Verified in 5/9 studies	
AMACR	Protein	Biopsy	+	Verified in 8/9 studies	
HSP60	Protein	Biopsy	+	Verified in 6/9 studies	
CDK7	Protein	Biopsy	+	Verified in 7/9 studies	
TPD52	Protein	Biopsy	+	Verified in 6/9 studies	

Figure 4: Biomarkers for Presence of Prostate Cancer. These biomarkers were quantified from tissue extractions at the time of radical prostatectomy. This table depicts which markers are clinically useful in differentiating between non-cancerous tissue and localized, benign prostate cancer. Source: [14]

Marker	Molecule Type	Sampled from	Up/Down-Regulated	Notes	Reference
Aurura Kinase A	Protein	Biopsy	+	Verified in 5/5 studies	14
EZH2	Protein	Biopsy	+	Verified in 5/5 studies	
Nucleoporin p62	Protein	Biopsy	+	Verified in 4/5 studies	
LAP2	Protein	Biopsy	+	Verified in 4/5 studies	
Ral A	Protein	Biopsy	+	Verified in 4/5 studies	
Ubc9	Protein	Biopsy	+	Verified in 4/5 studies	
Exportin1	Protein	Biopsy	+	Verified in 3/5 studies	
P16INK4A	Protein	Biopsy	+	Verified in 3/5 studies	
MSH2	Protein	Biopsy	+	Verified in 3/5 studies	

Figure 5: Biomarkers for Aggressiveness of Prostate Cancer. These biomarkers were quantified from tissue extractions at the time of radical prostatectomy. This table depicts which markers are clinically useful in differentiating between localized, benign tissue and metastatic tissue. Source: [14]

Despite these robust findings, the majority of the focus has been on detection of cancer (comparing non-cancerous samples with cancerous samples) and not testing for recurrence (comparing cancerous vs non-cancerous after chemical or radiation treatment). This is represented in Figure 6; most studies compare **A** and **B**, whereas few compare **C** and **D**. Serum

from patients with recurrence and serum with patients without recurrence will be assayed to determine the level of several biomarkers. Ideally, a discrepency between the recurrent and non-recurrent samples will provide a useful tool in assessing risk of recurrence from a patient after chemotherapy or radiation treatment.

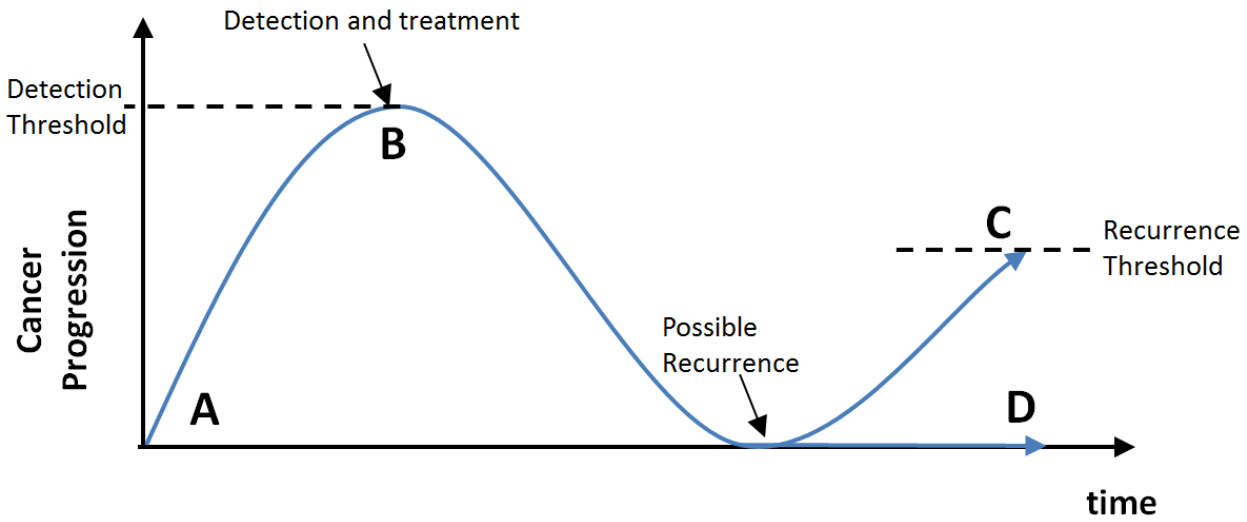

Figure 6: Strategies for Cancer Detection. (A) represents non-cancerous levels, **(B)** represents the levels required for the detection of cancer, **(C)** represents a secondary threshold for detecting recurrence, and **(D)** represents a successful treatment with no recurrence.

1.3 Serum Controls

In any analysis of serum biomarkers, phrases such as "upregulated" and "downregulated" are relative values for comparison. Usually, the level of such a biomarker is quantified over time, such that changes in the biomarker are compared or normalized to some previous value. Unfortunately, identifying risk of recurrence for prostate cancer is extremely important immediately after chemotherapy will occur, at a single time from a single test. It would be naïve to compare serum levels to a "pooled average" of every person, because the "normal" level of markers in serum is different from person to person. A better method would be to normalize the level of a biomarker to some standard and use the patient as his own control. Alkaline

phosphatase (ALP), which retains blood pH, is a strong candidate because its concentrations remain relatively stable in the blood throughout a person's lifetime.[17] Albumin, a protein involved in retaining serum oncotic pressure, is also relatively stable during a patient's lifetime and varies with certain diseases such as cancer.[18]

Marker	Use in Experiment
PSA (Prostate-Specific Antigen)	Gold Standard
SIM2 (Simple-Minded Homolog 2)	Biomarker of interest
ALP (Alkaline Phosphatase)	Serum Control

Figure 7: Selected Biomarkers for This Study. PSA is a gold standard, ALP will be a serum control, and SIM2 will be of specific interest.

The three biomarkers chosen for this specific study (Figure 7) were Prostate-Specific Antigen (PSA), Alkaline Phosphatase (ALP), and Single-Minded Homolog 2 (SIM2). PSA has long been utilized as a gold standard, ALP will represent a serum control, and SIM2 will be an experimental marker. It is expected that PSA and SIM2 will be higher in the patients with recurrence, and that the ALP will show no significant difference between groups. Relative levels will be calculated as:

$$Biomarker\ Level = \frac{Amount\ of\ Experimental\ Biomarker}{Amount\ of\ Reference\ Biomarker} \quad (1)$$

in which levels are reported as a fraction of some patient-specific serum control. Ideally, the levels of reference biomarker (alkaline phosphatase) will have a much lower range of variance than the experimental biomarkers themselves. The final step in the design is selection of the protocol to detect the markers.

2. Acoustic Wave Immunosensors

2.1 PiezoelectricAcoustic Waves

Piezoelectric materials directly convert mechanical stimuli into electrical stimuli, and vice versa. They are the link between mechanical and electrical phenomena and as such, a simple voltmeter can track changes in mechanical stimuli on the surface of the material. Mechanical signals in piezoelectric materials propagate either on the surface or through the material itself. Surface acoustic waves (SAWs) generate mechanical waves in the crystal parallel to the surface whereas bulk acoustic waves (BAWs) are designed to generate oscillations perpendicular to the surface of the material (Figure8). Such oscillations are recorded as voltages over time.

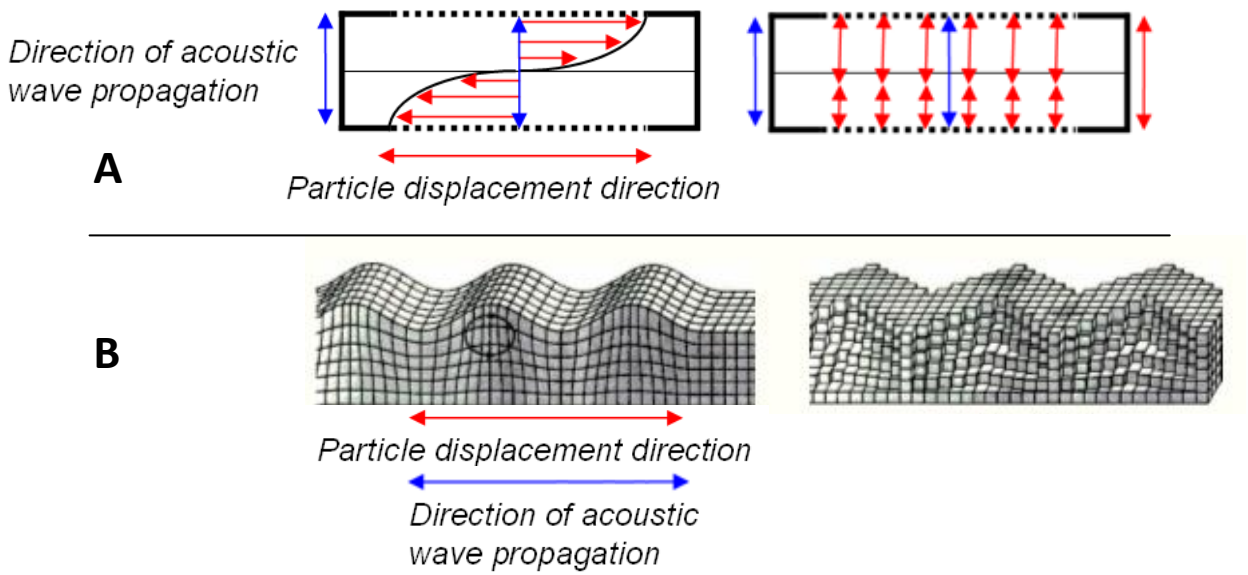

Figure 8: Bulk and Surface Acoustic Waves. Mechanically induced waves in piezoelectric materials convert physical crystal stretching into electric signals. **(A)** Bulk acoustic waves (BAW) generate mechanical waves into the material itself. **(B)** Surface acoustic waves generate mechanical oscillations across the surface. Modified from [19].

The voltage-varying signal can be explored using a real-time discrete Fourier transform (Equation 2) to decipher the frequencies of the signal over preselected time intervals:

$$X(\omega) = \sum_{n=-\infty}^{\infty} x[n]\, e^{-i\omega n} \tag{2}$$

The change in frequency of the resonator indicates a change in any of the multitude of surface boundary conditions, such as mass loading or shear stress, with great specificity.

SAW devices are quite large, must be cut from a perfect crystal, and are inherently difficult to integrate into microchips. Thus, BAW devices have become a better candidate for potential biosensors.[20] The resonant frequency of a BAW device is described by:

$$f_0 = \frac{v_a N}{2d}, N = 1,3,5, \ldots \tag{3}$$

Where v_a is the acoustic velocity, N is the mode number, and d is the film thickness. In 1959, Sauerbrey described the relationship between the mass loading on the sensor itself (Δm) with the observed electrical frequency change (Δf) [21]:

$$\Delta f = \frac{-f_0^2 \Delta m}{A\sqrt{\rho_q \mu_q}} \tag{4}$$

Where Δf is the change in frequency, f_o is the unloaded resonance frequency, Δm is the change in mass loading at the surface, A is the area of operation, ρ_q is the crystal mass density and μ_q is the crystal elastic stiffness. In addition, the equation governing liquid interactions with a surface was described in 1985[22]:

$$\Delta f = -f_0^{3/2} \sqrt{\frac{\eta \rho}{\pi \rho_q \mu_q}} \tag{5}$$

Where f_0 is again resonant frequency, η and ρ are viscosity and absolute density of the solution, and μ_q and ρ_q are shear stiffness and density of the BAW resonator.

2.2 Quantum Crystal Microbalance with Dissipation (QCM-D) Biosensor

The Quartz Crystal Microbalance (QCM), the most commonly used BAW sensor used today[20], was first described by Jacques and Pierre Curie in 1880.[23] The QCM is an ideal BAW sensor with air interface. The QCM, however, isn't an ideal biosensor due to its low frequency of operation (between 5 and 35 MHz).[20] Higher device operating frequencies lead to higher acoustic detection sensitivity.[24] A film bulk acoustic resonator (FBAR) contains layers of semiconducting film upon a standard BAW device platform to increase the internal resonant frequency well into the GHz range (Figure 9).[25]

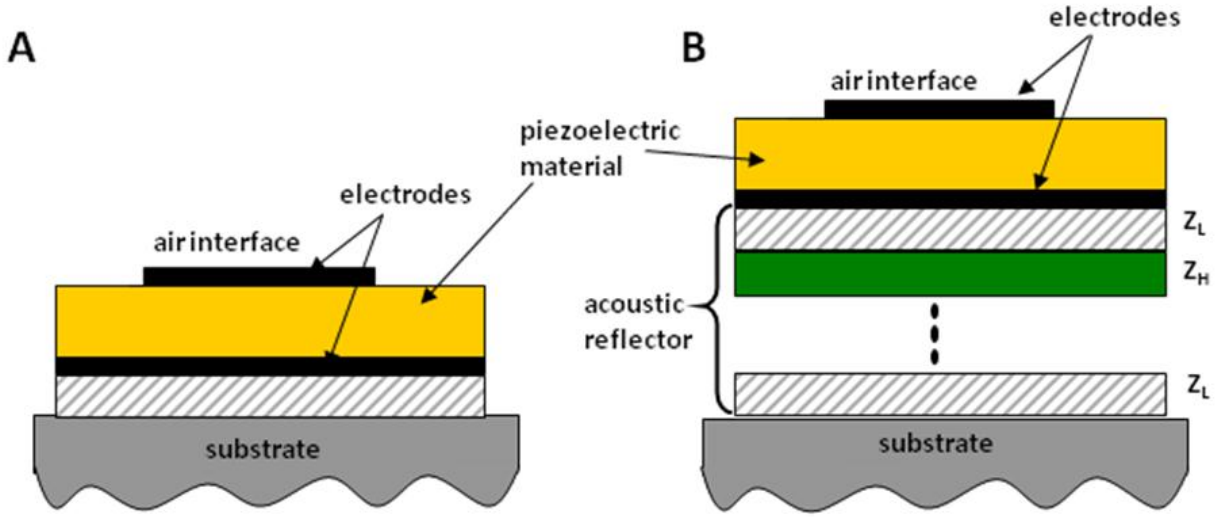

Figure 9: BAW Sensor and FBAR. Examples of QCM technology. **(A)** A standard QCM with a low operating resonant frequency. (B) A standard FBAR. Alternating film layers upon a QCM increase the internal resonant frequency of the BAW. Modified from [20].

The resonator becomes a biosensor when the surface material becomes inoculated with a layer of antibodies specific to a target antigen (Figure 10). The QCM was used for the first time as an immunosensor in 1976.[26] Binding events in the biolayer cause changes in the surface boundary conditions resulting in a change of the resonance frequency. Instead of measuring elusiveand indistinguishable changes at the surface, the resonator will now specifically measure immunobinding events in which the antibodies bind to target antigens in a liquid solution.

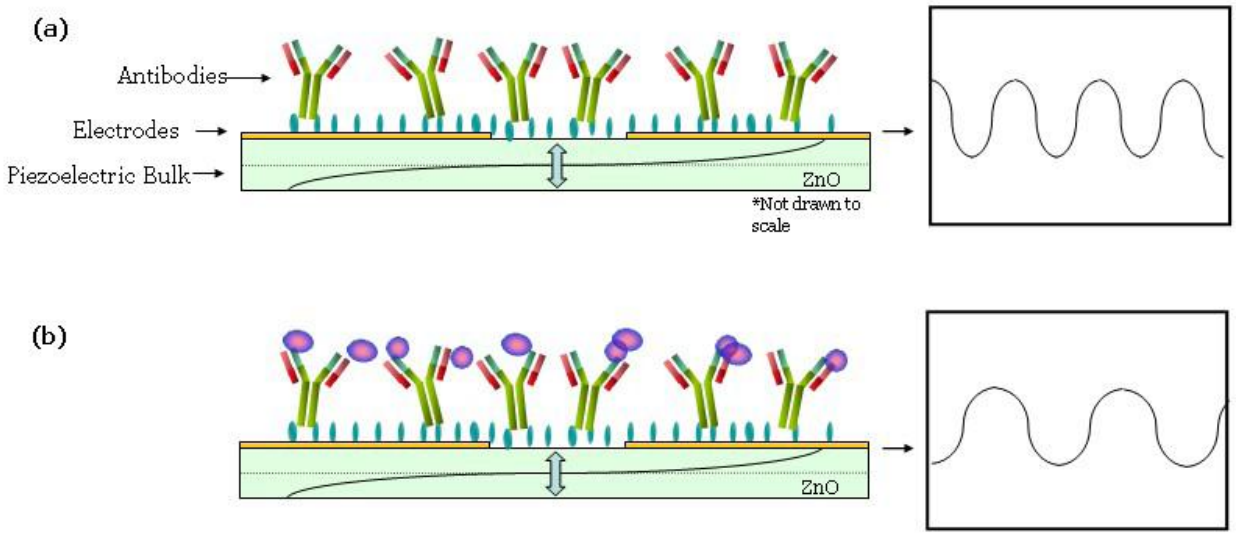

Figure 10: QCM Biosensor. Antibodies inoculated to the surface of the QCM are used to detect binding events indicative of a target molecule. **(a)** The QCM biosensor vibrates as an internal resonant frequency. **(b)** Once target antigens bind to the antibodies, surface perturbations and mass loading cause the internal resonant frequency to drop. Source[19].

The process of using antibodies ensures that the only mass loading events associated with the device are antigen immunoevents. However, extraction of mass data from observed frequency recordings can no longer be performed with the standard equations presented in Equations 2 to 5 because the biofilm adds additional physical characteristics which need to be mathematically addressed (Figure 11).

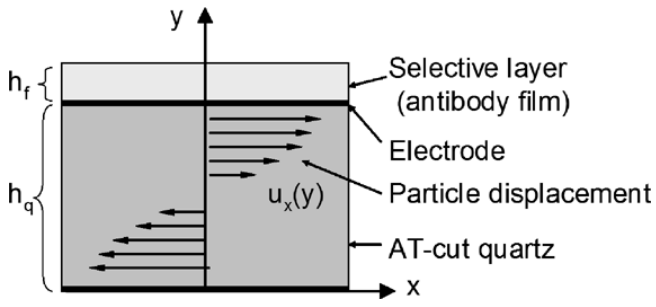

Figure 11: QCM Biosensor BAW model. Antibodies upon the h_f region introduce another mathematical boundary which needs to be addressed in the Sauerbrey model before mass calculations can be made. Source: [27].

In order to mathematically incorporate the biofilm layer, Hunt et al. developed a partial differential equation which incorporates the stiffness change of the QCM as a result of an immunobinding event with a target antigen:[28]

$$t\frac{\partial \Delta\omega}{\partial t} + \Delta\omega = \frac{\omega_u h_f}{\pi\sqrt{\rho_q \mu_q}} \times \left\{ -\omega_u \left[\Delta p - \frac{\Delta\mu}{V_s^2} \right] + j \left[\frac{\partial \Delta\rho}{\partial t} - \frac{1}{V_s^2} \times \frac{\partial \Delta\mu}{\partial t} \right] \right\} \quad (6)$$

where the subscript μ denotes the unperturbed field condition, f denotes the immobilized chemi-specific film, ω is the radian frequency, V_S is the velocity of the shear acoustic wave, and h_f is the height of the immobilized surface. Assuming that $\Delta\rho$, $\Delta\mu$, and $\Delta\omega$ do not change with time, Hunt's equation (6) reduces to:

$$\Delta f = \frac{-f_0^2 h_f}{A\sqrt{\rho_q \mu_q}} \left[\Delta\rho - \frac{\Delta\mu}{V_s^2} \right] \quad (7)$$

where μ_q and ρ_q are mass constants and mass loading is expressed as $\Delta m = \Delta\rho A h_f$.This equation is essentially the Sauerbrey Equation (4) in which the mass change Δm is expanded to include mechanical stiffness of the antibody layer. Individual sensors (Figure 12A) can be combined in series on a single chip (Figure 12B) to simultaneously infer 8 biomarker levels from a sample.

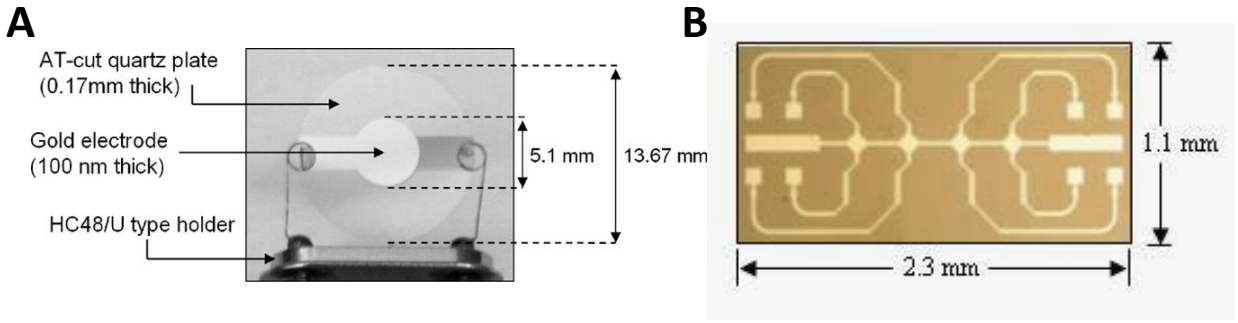

Figure 12: Individual Sensor and AcμRayMultisensor. Initial testing of individual biomolecules will take place on **(A)** QCM sensor pads. Eventually, once candidate biomarkers are validated, up to 8 markers can simultaneously be tested on the **(B)** AcμRay biomolecule sensor pad. Sources:**(A)**[27]**(B)**[29] .

RESEARCH CONDUCTED

1. Biosensor Design

The detection of specific serum proteins is the foundation for all biomarker analyses. Concerning cancer, biomarkers are often utilized for both diagnosis and prognosis of disease during risk assessment, screening, classification, tumor stage, tumor grade, of even risk of recurrence.[30] Inherent in this analysis is the sensitivity and selectivity of the method to detect the biomarker. A gold-standard biomarker detection method in clinical settings is the clinical ELISA[31], which is relatively tedious, expensive, and must be performed by trained personnel. In 1880, Quartz Crystal Microbalances (QCMs) were first described[23] and have since been used as chemical sensors due to their unique piezoelectric ability to translate changes in surface chemistry into electric signals. In 1959, it was determined that deposition mass on the QCM surface can be inferred from the drop in QCM resonant frequency using the Sauerbrey equation.[21] The resonator becomes a biosensor when the surface material becomes inoculated with a layer of antibodies specific to a target antigen. Ideally, the process of using antibodies ensures that the only mass loading events detected by the QCM resonator are antibody-antigen immunobinding events. In 1972, the QCM was first used as an immunosensor[26] and has since aided in the detection of explosives[32], bioterrorist threats[33], food and drug screening[34,35], tumor cell studies[36,37], and blood serum assays for human serum albumin[38] and cancer[39]. An additional aid in this detection is the QCM with dissipation (QCM-D), which allows for the simultaneous measurement of frequency shift and dissipation in order to infer deposition mass and viscoelasticity.[40]

Some organic molecules, such as alkanethiols, have the capacity to spontaneously chemisorb onto the gold QCM surface. Exploiting this technique allows for the formation of a nearly-perpendicular self-assembled monolayer (SAM) of carbon chains, to which antibodies can adhere.[41] Once the selective biofilm is created, the QCM-D sensor can be presented with antigen-containing solutions for electric detection. When the antigen does not naturally chemisorb to the gold QCM surface, it can be assumed that the entire electric frequency shift recorded from the QCM-D is due to an antibody-antigen binding event at the antibody's paratope. Fluorescein isothiocyanate (FITC) is an example of such a compound. However, if the antigen chemisorbs onto the gold surface spontaneously, the measured frequency shift of the sensor incorporates both specific binding at the antibody's paratope and the disorderly nonspecific binding onto the gold surface itself (Equation 8).

$$\Delta f_{Sensor} = \Delta f_{SpecificBindingOntoAntibody} + \Delta f_{Non-specificBindingAtSurface} \qquad (8)$$

This problem of simultaneous detection of specific and non-specific binding is alleviated with the use of a reference sensor: a second QCM-D sensor designed to detect a chemical which isn't in the antigen-containing solution (Figure 13). When both reference sensor and target sensor are exposed to the same antigen-containing solution, it is assumed that the nonspecific binding in each sensor is equal. Thus, the measurements from the reference sensor represents an accumulation of all non-specific binding on the target sensor and can be subtracted from the frequency shift of the target sensor to extrapolate the frequency shift due solely to theimmunobinding event (Equation 9). This approach also controls for the nonspecific binding of other molecules onto the QCM surface, which is useful when detecting a target antigen in a solution of complex biological media such as cell suspensions or serum.

$$\Delta f_{Specific\ binding} = \Delta f_{Target\ Sensor} - \Delta f_{Reference\ Sensor} \quad (9)$$

In order to detect a specific protein in a blood sample, for example, the use of a reference sensor for a non-organic molecule is paramount. FITC is an ideal choice for the antigen of the reference sensor because it typically isn't present in biological samples and it doesn't simultaneously bind to the gold surface or SAM.[28]

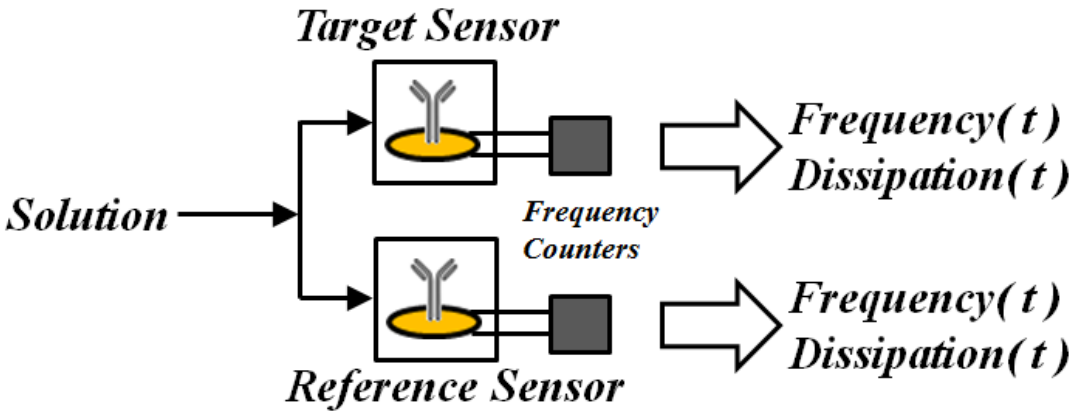

Figure 13: QCM-D Setup with Two Sensors in Parallel. The "target sensor" contains antibodies for a molecule of interest, whereas the "reference sensor" contains antibodies for a molecule known not to be present in the solution**.**

This project investigates the simultaneous incorporation of frequency and dissipation changes recorded from QCM-D target and reference sensors in order to infer mass and viscosity changes of immunobinding events on a QCM-D biosensor. In an effort to produce clinically-relevant findings towards designing biosensors for human serum, three antigen environments were investigated: a biologically inactive FITC solution, a recombinant bovine serum antigen (BSA) solution, and BSA-containing fetal bovine serum (FBS).The first set of experiments evaluates FITC as a candidate reference sensor and introduces the concept of antibody stiffening.

Next, a pure recombinant protein solution of BSA in PBS was detected with the parallel target/reference QCM approach. Fetal bovine serum diluted to the same concentration as the prior recombinant BSA solution was detected in order to demonstrate the approach's effectiveness in complex media. The next set of experiments was carried out to create a dose-response curve with the BSA in FBS. With these proof-of-concept experiments completed, human serum was utilized with the aforementioned biomarkers in order to detect biomarkers which may be indicative of prostate cancer recurrence.

2. Antibody Immobilization with QCM-D

2.1 Antibody Immobilization on the Biosensor

To clean the gold QCM-D sensors before use, they were first treated with UV/Ozone for 10 minutes. The sensors were then submerged in a 1:1:5 solution of NH_3:H_2O_2:H_2O at 75 ^{0}C for 5 minutes. After being rinsed with distilled water and air dried with nitrogen gas, the sensors were again treated with UV/Ozone for 10 minutes. The sensors were then mounted into individual flow chambers in the QSense E4 Flow Module system. In order to immobilize antibodies onto the surface of the QCM-D, a self-assembled monolayer (SAM) of alkane-thiols were created according to the reaction described in 1991.[42] The SAM and subsequent antibody reaction is depicted in Figure 14.

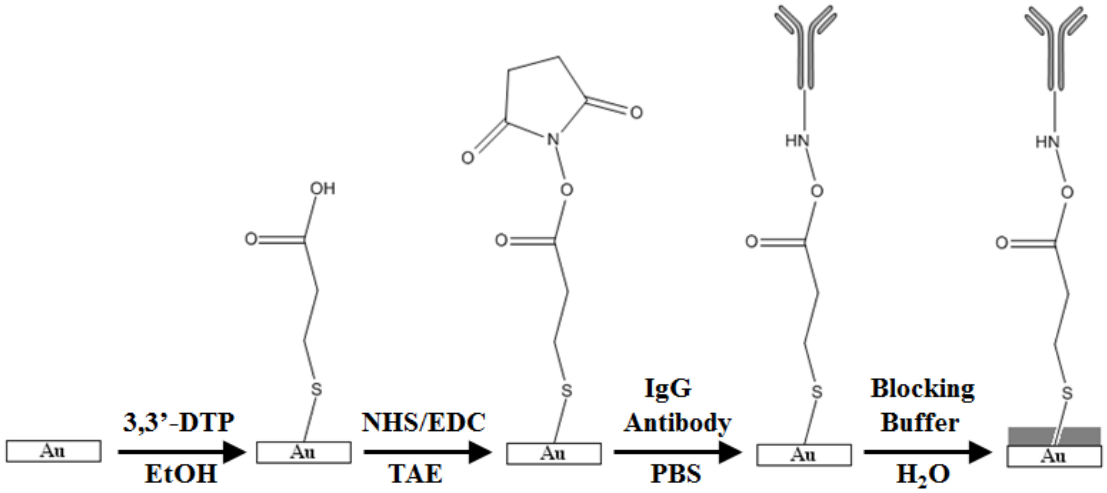

Figure 14:Antibody Immobilization Reaction. Alkanethiol bonds mount carbon chains to the gold sensor surface prior to a carboxylic acid activation and nucleophilic substitution in order to attach the antibody to the chain.

When transferring the antibody immobilization reaction protocol to the QCM-D, each reaction step in Figure 14 was implemented in three stages: buffer solution flowing at 100 µL/min, chemical solution in buffer flowing at 100 µL/min, and finally flowing buffer solution again. To adsorb the alkanethiol onto the sensor, ethanol was supplied before and after a solution

of 0.01 M 3,3'-Dithiodipropionic acid (3,3'-DTP) in ethanol. Distilled water and air were then applied through the chambers for 2 minutes each to wash the surface. Next, 0.655 g of 1-ethyl-3-(3-dimethylamino-propyl) carbodiimide (EDC) was dissolved in 5.0 mL of 1x Tris-Acetate-EDTA (TAE buffer) and added to a solution containing 0.765 g *N*-Hydroxysuccinimide (NHS) in 5 mL TAE to afford a 10.0 mL solution of EDC/NHS in TAE. To activate the carboxylic acid, the EDC/NHS solution was supplied to the flow chambers with TAE buffer flowing before and after. Water and air were once again used to wash the surface.

Phosphate-buffered saline (PBS) was then applied over each sensor and the flow was halted to allow for a static reading of PBS over each sensor. Mouse monoclonal IgG antibodies (20 µg/µL PBS) were then supplied to each sensor and allowed to adhere in a non-flowing manner to conserve stock antibody solution. For the target sensors, antibodies for the target antigen of interest were used. Likewise, for the reference sensor, the reference antibody was used. PBS was then flowed over the sensors and paused to obtain a final reading of frequency and dissipation. Ethanolamine (0.1 M) was used to block reactive sites which may have been inaccessible to the antibodies. Finally, in a similar volume-conserving fashion as that of the antibody solution, the test solutions, which contained target antigen, were flowed onto each sensor and allowed to rest, before and after their respective phosphate-buffered saline (PBS) buffer. The frequency and dissipation output of a typical reaction is shown in Figure 15.

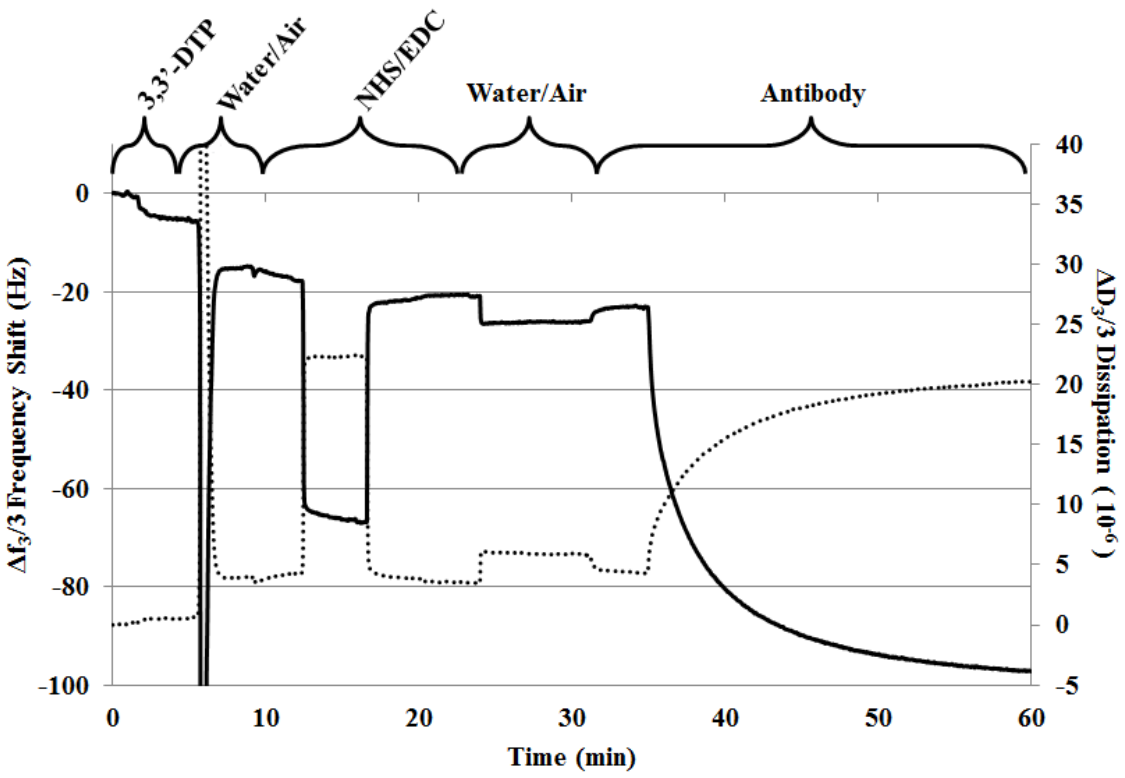

Figure 15: Antibody Immobilization on QCM-D. Antibodies inoculated to the surface of the QCM are used to detect binding events indicative of a target molecule.

2.2 Optimizing Antibody Concentration

Prior literature inoculates the sensors with 20 µg/mL antibody solution.[33,37] Because the QSense QCM-D flow chamber requires a minimum solution volume of 140 µL per sensor, investigations were carried out to determine if a lower concentration of antibody could be used with the same level of inoculation. Antibody solutions of 1 µg/mL, 5 µg/mL, 10µg/mL, and 20 µg/mL were utilized after the carboxylic activation step and the mass deposition was fairly correlative with the antibody concentration (Figure 16). Ultimately, the decision was made to use antibody solutions at the same concentration as prior literature (20 µg/mL).

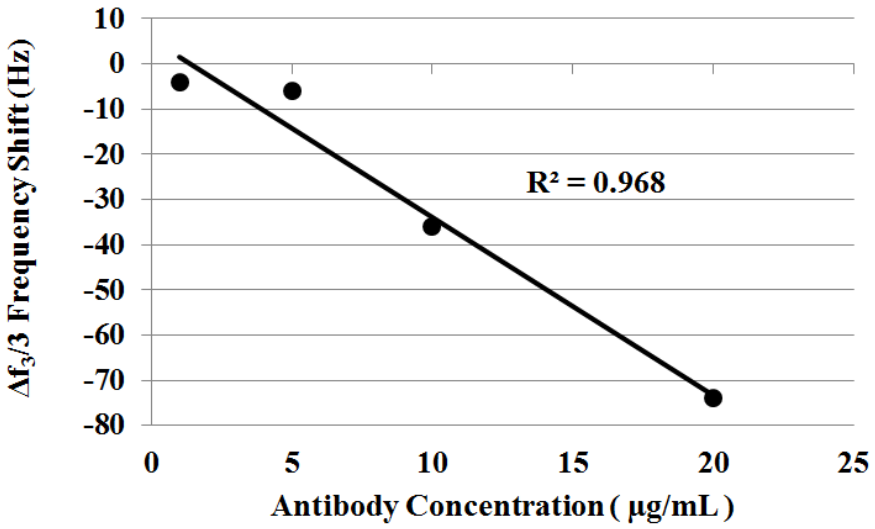

Figure 16: Antibody Deposition vs. Concentration. Antibodies inoculated to the surface of the QCM at different concentrations and showed a direct relationship with mass deposition (negative frequency shift).

3. Immunospecific Detection of Target Molecules

3.1 Inorganic Molecules in Saline

FITC has previously been used as a reference sensor in complex biological media.[37] The Saurbery equation (Equation 4) predicts that binding of the 389.4 Da FITC antigen onto the 150 kDaIgG αFITC antibody should elicit a slightly negative frequency shift. However, the immunobinding event actually induces a dramatically positive frequency shift in a dose-dependent fashion (Figure 17). Extraction of ultimate mass loading data from these observed frequency recordings cannot be directly inferred with the Sauerbrey equation because the biofilm adds additional physical characteristics which need to be mathematically addressed.

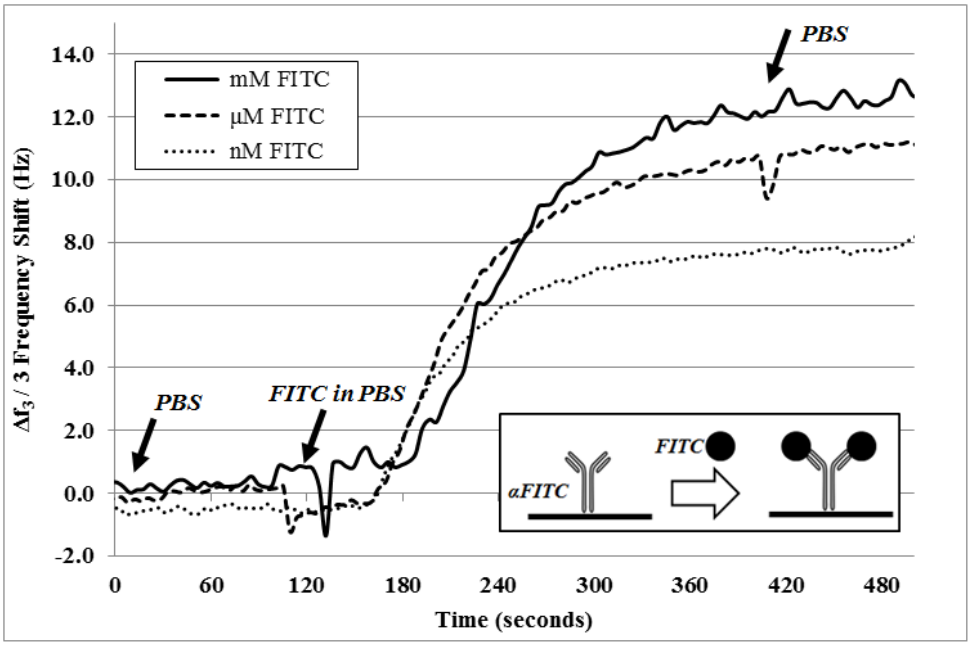

Figure 17: FITC Binding onto QCM-D Biosensor. The positive frequency shift elicited by the FITC – αFITC immunoreaction displays a dose-dependent response

In order to mathematically incorporate the antibody biofilm layer into the QCM model, Hunt et al. developed a partial differential equation which incorporates the stiffness change of

the QCM as a result of an immunobinding event with a target antigen (Equation 6).The data presented in Figure 17 fit this model; FITC concentration induces increases in frequency shift in a dose-dependent fashion.It has previously been reported that antibodies increase their stiffness after an immunobinding event.[43] Because of the miniscule size of FITC in comparison to the antibody, the measured increase in frequency shift must be due, in part, to the stiffness change.

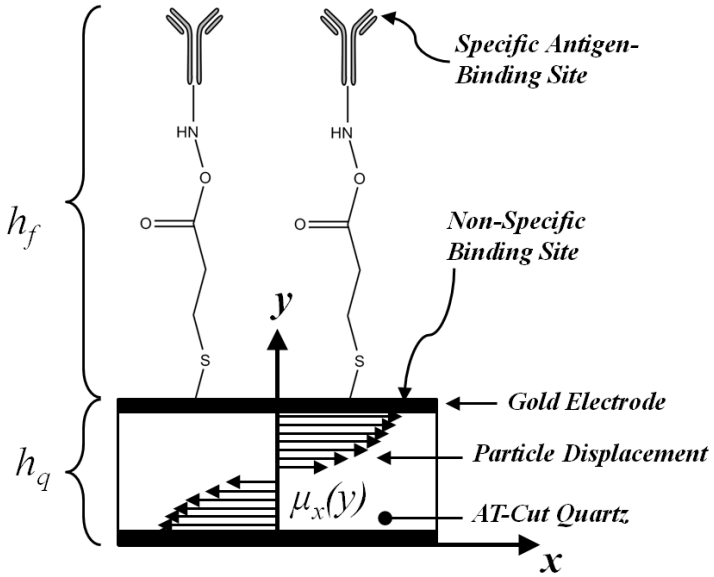

Figure 18: QCM-D Immunosensor Model. The known biofilm layer in the h_f region acts as a spring. Binding of antigen to antibody changes the biofilm's resonant frequency, ultimately affecting the frequency of the BAW.

3.2 Serum Proteins in Recombinant Solution

In order to investigate towards clinically relevant findings, several biological media were utilized for protein detection. Bovine serum albumin (BSA) is a highly concentrated protein in fetal bovine serum (FBS). The first biological experiment was an investigation of recombinant BSA protein in PBS buffer. A parallel-flow QCM-D approach was utilized, with αBSA antibodies on the target sensor and αFITC antibodies on the reference sensor. After the formation of the SAM and antibody layer, a 1 mg/mL solution of BSA in PBS was then applied to each of the sensors and allowed to reach steady state (Δf < 1 Hz/min). The resulting time-varying

frequency shifts of the target and reference sensors are depicted in the top two data series of Figure 21.

The model (Figure 18) represents the two generalized areas where BSA could have bound in an experimental situation: the gold surface and the antibodies themselves. Despite the fact that there is clearly a drop in frequency for both sensors, the results mirror those of the FITC trials in that the difference in frequency shift (Equation 7) is a positive change. Using the sensors, it was determined that a 1 mg/mL concentration of BSA elicits a frequency shift of 3.075917 Hz on the third harmonic. This positive change indicates the change in stiffness term of Equation 7 is greater than the mass deposition term.

3.3 Blocking Biosensor Surface of Non-Specific Binding

Some publications utilized ethanolamine as a blocking agent, though its efficacy in blocking large amounts of nonspecific serum is unknown. A single set of experiments showed the extent of non-specific binding of FBS (Figure 19). First depicted is the frequency drop due to FBS binding onto the gold sensor surface without any prior treatment; no antibodies or thiol chains. The next bar represents FBS binding after αFITC antibodies were inoculated. As expected, the FBS bound less because the antibodies presumably took up space on the sensor surface and sterically hindered the binding sites. The final bar depicts the same reaction (FBS onto αFITC), though an additional step with ethanolamine was supplied to the surface prior to FBS treatment. As expected, the ethanolamine prevented FBS binding. However, the fact that the non-specific binding is being subtracted out makes this step redundant in the overall scope of the experiment. As such, ethanolamine was not used in any subsequent serum experimentation.

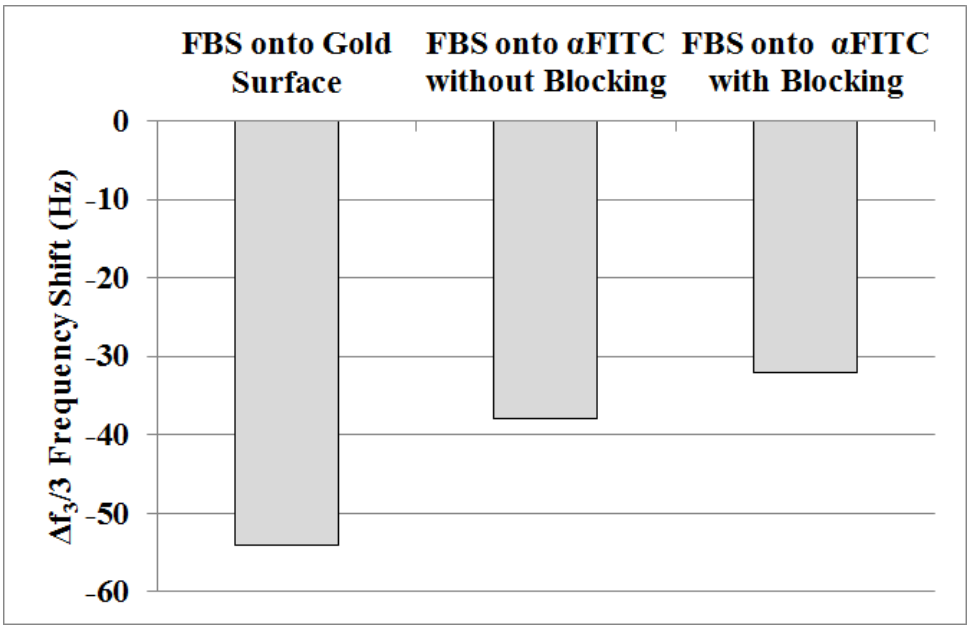

Figure 19: Blocking the Surface with Ethanolamine. (Left) FBS bound the most when it was presented with a fresh sensor. **(Center)**Anti-FITC antibodies removed some of the binding sites and less FBS bound non-specifically to the surface. **(Right)** Treating the anti-FITC layer with ethanolamine further reduced non-specific FBS binding.

3.4 Serum Proteins in Blood Serum

To determine the extent that a reference sensor can account for all non-specific binding, a solution of diluted FBS was analyzed with the αBSA target sensor and αFITC reference sensor (Figure 20). The concentration of BSA in FBS is roughly 17 mg/mL, so a 1:20 dilution brings the concentration nearly equivocal to that of the recombinant protein solution. Because many more proteins bound to the surface of the reference sensor with the diluted FBS trial than the recombinant BSA experiments, the frequency drop is much greater. However, the sensors in tandem were extremely effective in isolating the antibody stiffness change. In the diluted FBS sample, a 1 mg/mL BSA concentration causes a 3.10951 Hz frequency shift. Repeated trials showed there was no significant difference in BSA frequency shift, whether from recombinant solution or diluted serum.

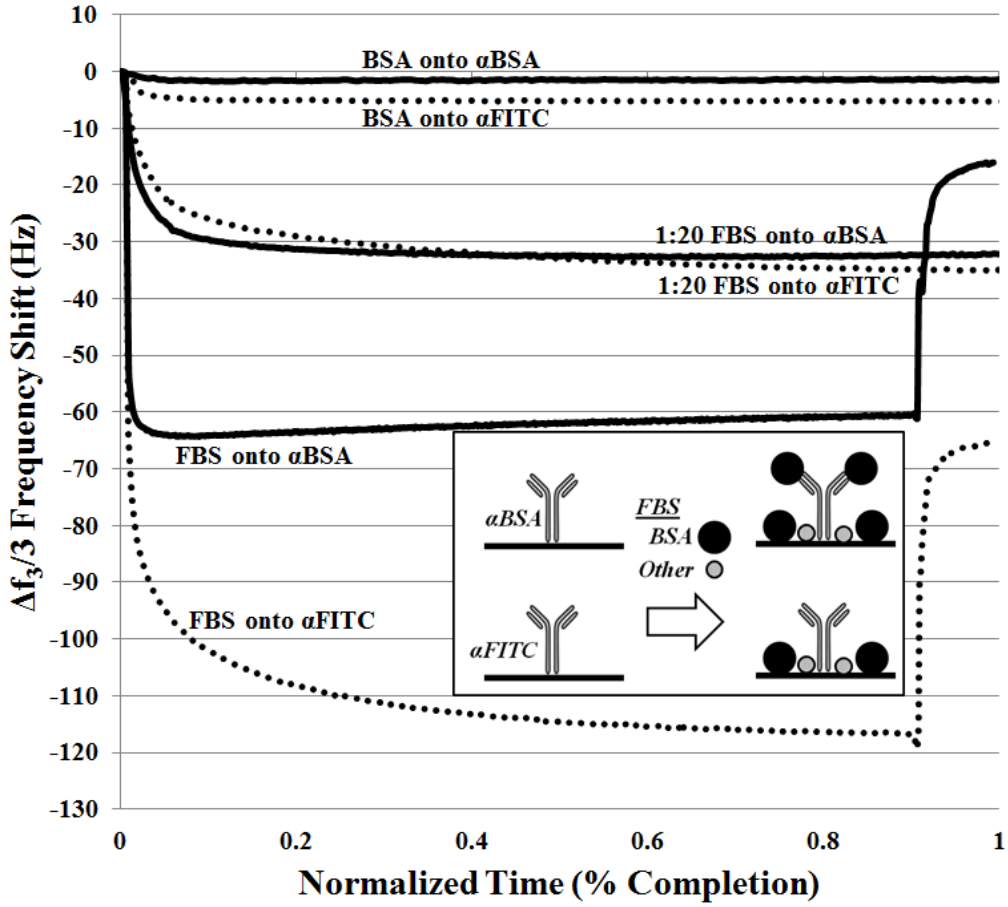

Figure 20: Detection of BSA in Recombinant Solution and FBS. Realtime frequency shifts of the third harmonic due to adsorption of BSA onto target and reference sensors. At time = 0, the BSA-containing solution (either recombinant BSA or FBS) was introduced to the two sets of sensors. At t = 0.9, buffer was introduced. In the case of BSA and 1:20 FBS, the changes in viscosity were not noticeable with the addition of buffer. However, there was a large frequency shift in the case of pure FBS.

To make use of these data in a diagnostic setting, it would be useful to determine if the frequency shift of a 1:20 dilution of FBS was merely 1/20th of the frequency shift of a pure sample of FBS. To investigate the ability to extrapolate sensor frequency shifts to other concentrations, a pure solution of FBS was analyzed for BSA content in the same fashion as before; αFITC reference sensor and αBSA target sensor. Although the recorded antibody frequency shift (49.8134 Hz) was within an order of magnitude of the theoretical multiple of diluted FBS frequency shift (3.10951 Hz × 20 = 62.1902 Hz), experimentation only yielded a frequency shift of 80.098% magnitude. A summary of frequency shifts from the various

environments is compiled in Figure 22. There are a number of reasons why the extrapolation was not more coincident. Namely, the system is not linear.

Until now, the assumption has been made that specific and non-specific frequency changes are independent of one another. In actuality, this can neither be confirmed nor refuted. Possible energy loss due to viscoelastic friction may contribute to nonlinear behavior, and interfacial slippage may affect frequency shift.[44] Additionally, it is currently impossible to measure both frequency and stiffness changes independently in order to infer deposition mass with Hunt's steady state time perturbation equation. Unlike traditional QCM devices, the QCM-D introduces a roundabout way of evaluating changes in stiffness: viscoelasticity modeling.

3.5 QCM-D Viscoelasticity

The QSense QCM-D E4 Flow Module was utilized in all experimentation because it can simultaneously measure frequency (Equation 4) and dissipation (Equation 10) changes in order to infer mass and viscosity changes at the surface of the sensor. As previously mentioned, it is necessary to flow a buffer solution before and after a solution which contains a compound which will augment the surface of the QCM-D. For example, the first step in the SAM construction is the deposition of 3,3'-DTP (Figure 14). This slight –3.5 Hz frequency shift correlates to 50.0 ng of mass added to the surface of the sensor, in the form of ~ 2.86×10^{14} alkane-thiol chains. It is assumed that the IgG antibody is 5.9 nm × 13.1 nm × 14.3 nm, with a molecular mass of 150 kDa.[45] These measurements, along with chemical properties of the known biofilm (Figure 21), were incorporated into the viscoelastic models within QSense's software in order to conduct viscoelasticity measurements.

$$\Delta f = \frac{-f_0^2 \Delta m}{A\sqrt{\rho_q \mu_q}} \tag{4}$$

$$D = \frac{E_{Dissipated}}{2\pi E_{Stored}} \tag{10}$$

Molecule	Molecular Mass	Base Area (nm^2)	Height (nm)	Density (ng/nm^3)
IgG	150 kDa	77.29	14.3	225.443×10^{-13}
Au-SAM	98.10 Da	0.04206	0.9057	4.27×10^{-12}
Au-SAM-IgG	150 kDa	77.29	15.2	225.443×10^{-13}

Figure 21: Biofilm Properties. Mass, area, height, and density were calculated from known bond lengths and assumptions from the biofilm model (Figure 19).

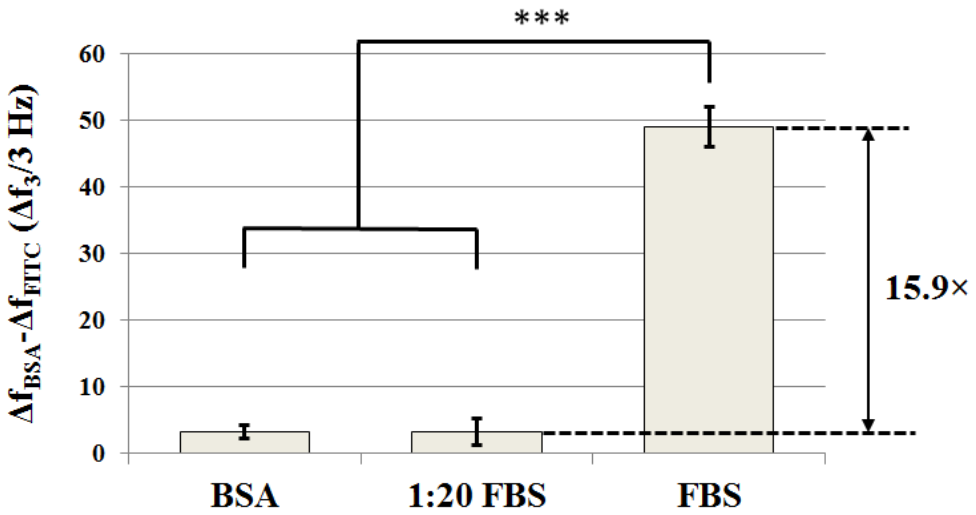

Figure 22:Frequency Shifts due to BSA Binding. The 1:20 dilution of FBS contains the same concentration of BSA as the recombinant BSA solution. Because the dilution factor (1:20) does not match the multiple difference in frequency (15.9), the system is relatively non-linear.

The QSense QCM-D software utilizes multiple simultaneous harmonics in its Voight viscoelastic model to correct for errors in the Saurbrey model and even to determine viscoelastic properties as well. The known chemical structure of the biofilm (Figure 18) was utilized to calculate a series of parameters (Figure 21) for use in the viscoelasticity model in the QSense QTools program. The recombinant BSA solution, 1:20 FBS dilution, and pure FBS solutions

which were previously analyzed for frequency shifts were also used to infer changes in surface viscoelasticity. In concordance with the isolation of specific antibody changes, the change in reference sensor viscoelasticity was subtracted from the target sensor viscoelasticity (Figure 23). Unlike the frequency normalization, the viscoelastic model is much more sensitive to mass accumulation at the surface than is the mere frequency shift. At present, this viscoelasticity fits a trend for antibody stiffness, but its direct integration into Hunt's equation (Equation 7) is not possible.

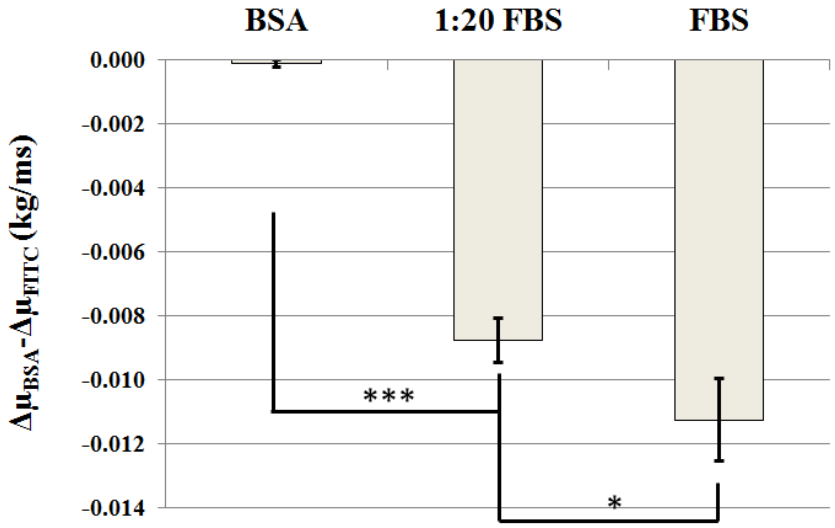

Figure 23:Viscoelasticity Shifts due to BSA Binding. The 1:20 dilution of FBS contains the same concentration of BSA as the recombinant BSA solution, yet all chemical environments were shown to have statistically different differences in viscoelasticity.

4. Detection of Recurrence Biomarkers in Human Serum

Patient serum was acquired from the Emory University Serum Bank in 150 μL aliquots and 2 cohorts: recurrent prostate cancer and non-recurrent prostate cancer (Figure 24). All ten patients had their blood drawn after a successful chemotherapy. Next, the serum was placed in a -80 ºC freezer. Four years later, serum was stratified based on whether the patients had developed recurrent prostate cancer during those prior 4 years.

Recurrent		
CFC#	**TID**	**# of vials**
281	2755	7
14	4254	5
218	415	3
114	1824	3
254	10251	3

Non-Recurrent		
CFC#	**TID**	**# of vials**
23	4316	10
20	SB 780	7
16	4289	6
22	4330	5
12	4291	4

Figure 24: Human Serum Identification. Human serum was acquired in 150 μL aliquots. 5 samples were taken from patients with recurrent prostate cancer, and 5 were taken from patients with non-recurrent prostate cancer.

Sample number 14, from the recurrent cohort, was analyzed on the QCM-D biosensor. One sensor had a reference antibody (αFITC), whereas the remaining 3 sensors contained antibodies for SIM2, ALP, and PSA (Figure 7). The differences in frequency drops due to the various antibodies was negligable, meaning that an approximately equivalent amount of IgG antibody bound to each sensor. Once the sensors had their respective antibodies, a 1:10 diluted sample of Human Serum #14 (diluted in PBS) was introduced to each sensor (Figure 25). As expected, the anti-FITC reference sensor had the greatest drop in frequency. SIM2 and ALP had slight increases in frequency due to antibody stiffening, and PSA had a much higher detection.

Aside from the mere difference in frequency before and after the serum sample, an interesting point is the slope of each graph. A steep drop is equivalent to faster binding kinetics:

the greater the binding per unit of time. The most overwhelming example of this is the PSA; the antibodies for PSA grabbed the PSA in the sample within minutes and was almost immediately at steady state. A more gradual binding curve is indicative of non-specific binding because the reaction relies on nonspecific binding patterns. The non-specific binding of serum proteins onto the αFITC reference sensor in Figure 26 resembles the non-specific binding of antibodies onto the alkane-thiol layer during antibody immobilization (Figure 15). A steep curve is likely indicative of immunobinding events.

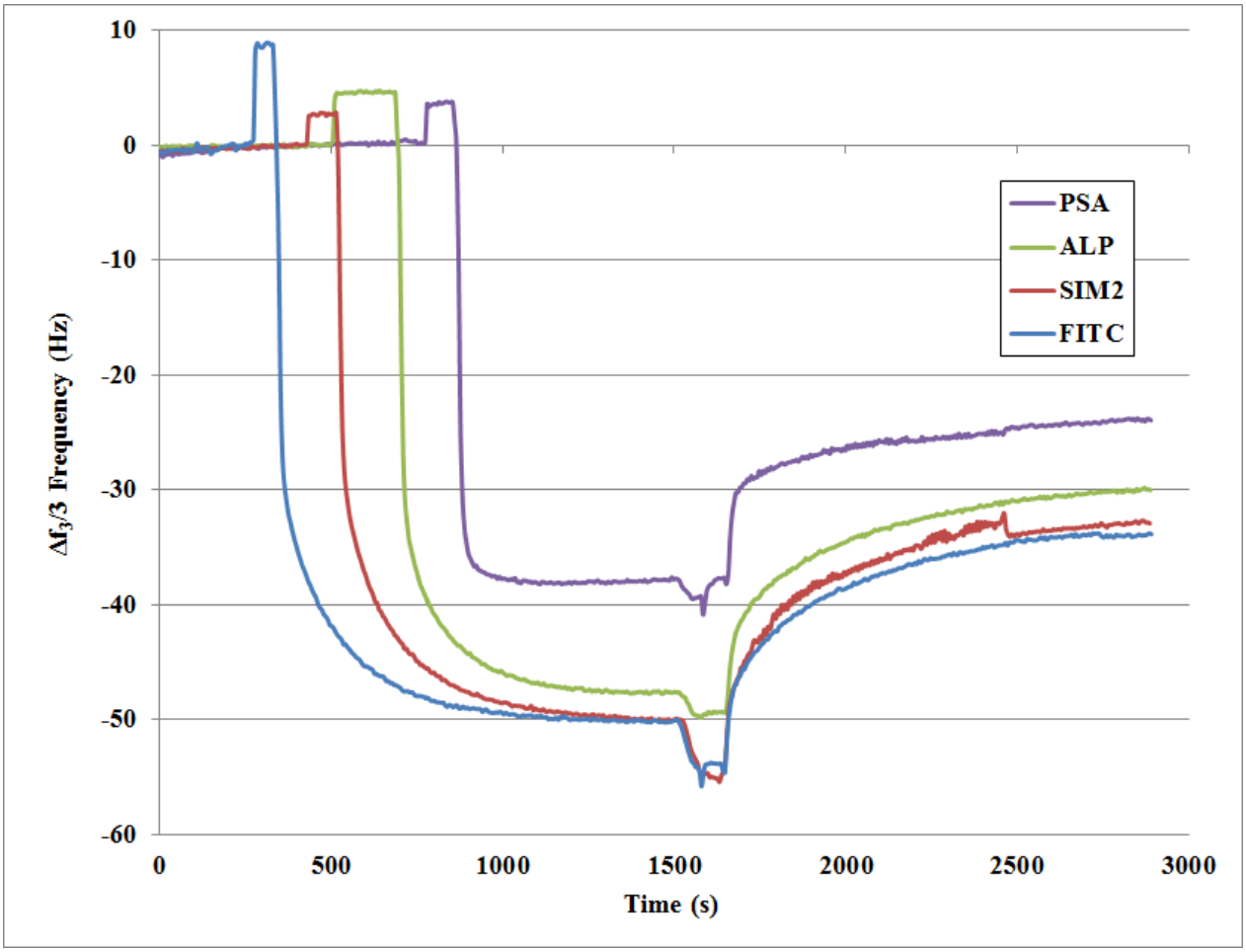

Figure 25: Detection of Recurrent Biomarkers in Human Serum. Diluted human serum sample 14 was presented onto four QCM-D immunosensors inoculated with antibodies for FITC, SIM2, ALP, and PSA. As expected, the FITC drop was the greatest. Interestingly, the PSA drop was extremely steep, indicating rapid immunobinding kinetics unlike the slow binding pattern of non-specific binding onto the surface.

Sample 281, like sample 14, is from the 'recurrent' cancer cohort. To investigate the difference between samples from the same group, the experiment was repeated for sample 281. Subtracting the frequency shift due to the reference sensor allowed for the comparison of biomarker levels at the antibody (Figure 26). Interestingly, SIM2 levels were extremely similar. These experiments will surely be repeated for all serum in Figure 24.

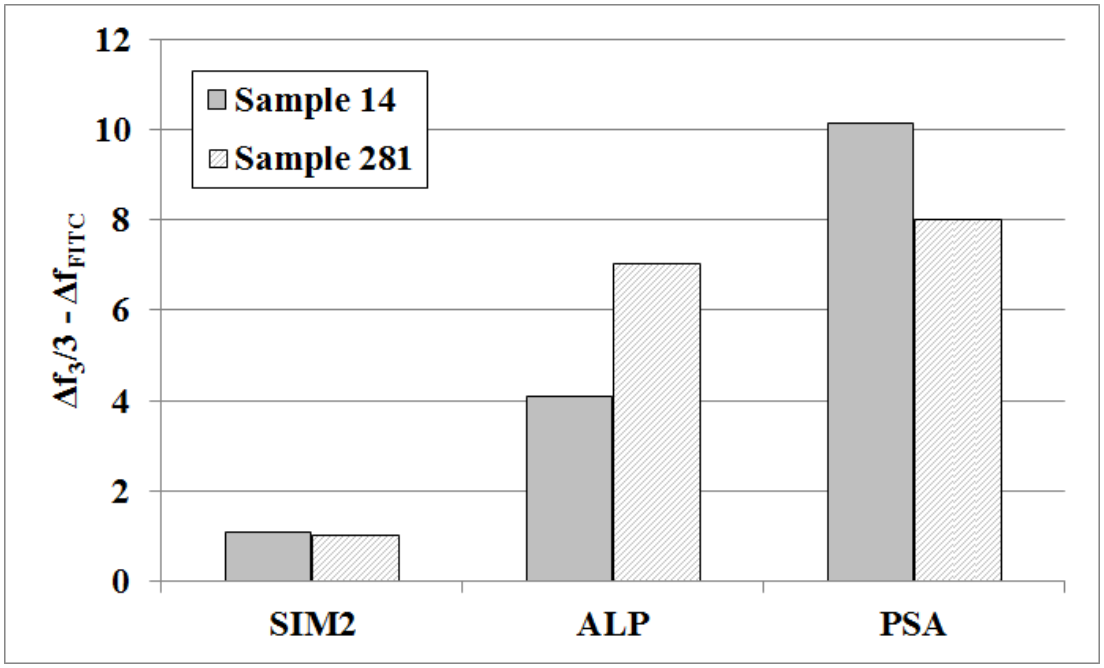

Figure 26:Biomarker Levels in Recurrent Prostate Cancer. Diluted human serum sampleswere placed onto QCM-D immunosensors inoculated with antibodies for FITC, SIM2, ALP, and PSA. The FITC frequency shift was subtracted in order to isolate frequency shift due solely to the biomarker of interest.

QCM-D biosensors were constructed and utilized in a two-sensor approach to isolate frequency, dissipation, and viscoelasticity changes while antigens adsorbed onto the surface. The reference sensor normalizes for all non-specific protein binding at the surface of the sensor, while the target sensor additionally incorporates changes in surface chemistry due to the immunobinding event. The uniquely positive frequency shift of FITC binding to its antibody lead

to the incorporation of mass and stiffness into the Sauerbrey frequency shift model for a series of BSA detection experiments in both recombinant protein and FBS solutions.

These studies showed the best designs to utilize QCM-D biosensors in a clinical environment with repeatable results incorporate parallel target and reference sensors which can infer a difference in frequency shift. The proof-of-concept testing with various inorganic, organic, and complex media allowed for the construction of a sophisticated biosensor capable of detecting various biological proteins in human serum. Repeated trials will surely indicate whether SIM2 is capable of differentiating between recurrent and non-recurrent prostate cancer serum samples. The majority of this work, however, is independent of the biomarker itself. These experiments optimized the design of a sensor to detect any biomarker which has an antibody available.

APPENDIX: QCM-D Protocol

1. **Clean Sensors**
    a. Place 4 sensors in the UV-Ozone Chamber for 10 minutes
    b. While in the chamber, make a solution of 5:1:1 H_2O:H_2O_2:$NH_3$and place the beaker on a hot plate at 75 ºC
    c. Once the sensors are done in the chamber, use the tweezers to pick up each sensor and place it into the plastic holder
    d. Place the holder into the water/ammonia/peroxide solution for 5 minutes
    e. Remove the holder from the solution and rinse with DI water and use N_2 to dry the sensors
    f. Once dry, remove from holder and place in UV/Ozone again for 10 minutes
    g. Use tweezers to place sensors back in holder and carry to QCM-D

2. **Place Sensors in QCM-D Flow Chambers**
    a. Flip each sensor chamber upside down and twist off the covers
    b. Use the tweezers to individually load the sensors into each chamber
    c. Twist on each cover, flip over the chamber into its place, and use lever to lock in
    d. Turn on QSense QCM-D machine

3. **Calibrate the Sensors**
    a. Begin flowing ethanol (EtOH) at 100 µL/min (0.100 on pump)
    b. Once EtOH has hit each chamber, open "QSoft" software
    c. Click on "Setup Acquisition"
    d. Make sure that "all 4 sensors have same resonant frequency" and "Low Noise" are selected
    e. Click "Find All" and wait a few minutes for the device to acquire baseline resonant frequencies
    f. Next, click "Begin Acquisition"
    g. Wait 2 minutes. Sometimes, the frequencies (blue) or dissipations (red) will vary with time, trending up or down. Obviously there's nothing going on at the surface, so you must recalibrate. Click "stop acquisition" and repeat from step 3C.

4. **Immobilizing the Antibodies**
    a. With Ethanol still flowing, hit "stop" on the pump and place the inlet tubes into a vial of the "3,3'-DTP in EtOH" and begin suction. MAKE SURE THERE ARE NO AIR BUBBLES.
    b. Once the frequency stabilizes (~10 minutes), begin to flow ethanol again to attain a final frequency reading.
    c. Next, flow TAE buffer and wait for it to stabilize
    d. Create the NHS/ECD in TAE solution. The NHS is pre-made, but the ECD must be made fresh each test. Retrieve the EDC container from the -80 ºC freezer and measure the solid. Add TAE, mix well, and add NHS. Once the frequency from the TAE is stabilized, flow the NHS/ECD in TAE solution
    e. Once stabilized, flow TAE again.

f. Next, flow PBS
g. Create antibody solutions by performing 1:10 dilutions and 1:20 dilutions of stock antibody solutions (marked on paper).
h. Next, add the antibody solutions individually and let the 140 μL rest on the sensor; stop flow once the solution fully enters the chamber.
i. Perform this for the other 3 sensors; each with its own antibody.
j. Wait ~45 minutes
k. Flow PBS on all sensors. At this point, each sensor has the antibody-alkane-thiol chain bound to its surface

5. Addition of antigen-containing solution (serum, etc)

a. Once PBS is stabilized, individually add serum (or whatever else) in the exact same fashion as the antibody; one at a time and carefully
b. Once serum is resting on each sensor, wait ~20 minutes for binding. Make sure to completely let the system rest until the final resonant frequency is found.
c. Once the sensors have stabilized, flow PBS on the sensors to acquire the final resonant frequency.

6. Cleanup

a. Save all data
b. Flow water for a few minutes (can do up to 200 μL/min to save time)
c. Flow the hellmanex solution
d. Flow water again
e. Flow air briefly to remove all liquid from tubing
f. Turn off pump and unclick each plastic holder on pump (no pressure on tubes)
g. Turn off QSense Machine
h. Flip over each chamber, twist off covers, and use tweezers to place sensors in the plastic holder
i. Rinse sensors with methanol, then water, then dry with N_2
j. Store sensors and clean up everything else

REFERENCES

1. Prostate Cancer. 2010; http://www.cancer.org/Cancer/ProstateCancer/DetailedGuide/prostate-cancer-key-statistics. Accessed July 2, 2010.

2. Kleinsmith LK. *Principles of Cancer Biology*. 1 ed. San Francisco, CA: Pearson Benjamin Cummings; 2006.

3. Weinberg DHaR. The Hallmarks of Cancer. *Cell.* 2000;100:57-70.

4. TA Stamey NY, AR Hay, JE McNeal, FS Freiha, and E Redwine. Prostate-specific antigen as a serum marker for adenocarcinoma of the prostate. *The New England Journal of Medicine.* 1987;317:909-916.

5. Stephen D. Mikolajczyk KMM, Lisa S. Millar, Abhay Kumar, Mohammad S. Saedi, Janice K. Payne, Cindy L. Evans, Carlton L. Gasior, Harry J. Linton, Philip Carpenter, and Harry G. Rittenhouse. A Truncated Precursor Form of Prostate-specific Antigen Is a More Specific Serum Marker of Prostate Cancer. *Cancer Research.* 2001;61.

6. Eddy SL, Grant WC, Bruce JT, et al. EPCA-2: A Highly Specific Serum Marker for Prostate Cancer. *Urology.* 2007;69(4):714-720.

7. Cohen DP, TA Stamey, KF Wilson, DR Clemmons and RG Rosenfeld Elevated levels of insulin-like growth factor-binding protein-2 in the serum of prostate cancer patients. *Journal of Clinical Endocrinology & Metabolism.* 1993;76:1031-1035.

8. Gunjan Malik MDW, Saurabh K. Gupta, Michael W. Trosset, William E. Grizzle, Bao-Ling Adam, Jose I. Diaz and O. John Semmes. Serum Levels of an Isoform of Apolipoprotein A-II as a Potential Marker for Prostate Cancer. *Clinical Cancer Research.* 2005;11.

9. Laura P. Hale DTP, Luis M. Sanchez, Wendy Demark-Wahnefried and John F. Madden. Zinc α-2-Glycoprotein Is Expressed by Malignant Prostatic Epithelium and May Serve as a Potential Serum Marker for Prostate Cancer. *Clinical Cancer Research.* 2001;7.

10. P Garnero NB, J Zekri, R Rizzoli, R E Coleman, and P D Delmas. Markers of bone turnover for the management of patients with bone metastases from prostate cancer. *British Journal of Cancer.* 2000;82(4):858-864.

11. Alka Jain DAM, Larry W. Fisher, Elizabeth B. Humphreys, Leslie A. Mangold, Alan W. Partin and Neal S. Fedarko. Small Integrin-Binding Proteins as Serum Markers for Prostate Cancer Detection. *Clinical Cancer Research.* 2009;15.

12. Edelson E. PSA Test Remains a Viable Tool - For Now. *Health Day News* 2009; http://www.pcf.org/site/c.leJRIROrEpH/b.5801021/k.1C24/PSA_Test_Remains_a_Viable_Tool_8211_For_Now.htm. Accessed Nov 29, 2009.

13. Bruce Alberts AJ, Julian Lewis, Martin Raff, Keith Roberts, and Peter Walter. *Molecular Biology of the Cell*. 5 ed. New York: Garland Science; 2008.

14. Varambally S, Yu J, Laxman B, et al. Integrative genomic and proteomic analysis of prostate cancer reveals signatures of metastatic progression. 2005;8(5):393-406.

15. TABACK B, O'DAY SJ, HOON DSB. Quantification of Circulating DNA in the Plasma and Serum of Cancer Patients. *Annals of the New York Academy of Sciences.* 2004;1022(Circulating Nucleic Acids in Plasma/Serum III and Serum Proteomics):17-24.

16. Banyard J, Zetter BR. The Role of Cell Motility in Prostate Cancer. *Cancer and Metastasis Reviews.* 1998;17(4):449-458.

17. Charles H, Clarence VH. Studies on Prostatic Cancer: I. The Effect of Castration, of Estrogen and of Androgen Injection on Serum Phosphatases in Metastatic Carcinoma of the Prostate* * This investigation was aided by a grant from the Committee on Research in Problems of Sex, the National Research Council. *The Journal of urology.* 2002;168(1):9-12.

18. Andrew Phillips AGSaPW. ASSOCIATION BETWEEN SERUM ALBUMIN AND MORTALITY FROM CARDIOVASCULAR DISEASE, CANCER, AND OTHER CAUSES. *The Lancet.* 1989;334(8677):1434-1436.

19. Corso C. *Theoretical and Experimental Development of a ZnO-Based Laterally Excited Thickness Shear Mode Acoustic Wave Immunosensor for Cancer Biomarker Detection*. Atlanta: School of Biomedical Engineering, Georgia Institute of Technology; 2008.

20. Wathen A. *The Development of Acoustic Wave Biosensor Arrays for the Simultaneous Multiplexed Detection of Multiple Prostate Cancer Biomarkers*. Atlanta: School of Electrical and Computer Engineering, Georgia Institute of Technology; 2009.

21. Sauerbrey G. Use of quartz vibrator for weighing thing films on microbalance. *Z. Phys.* 1959;155:206-210.

22. Kanazawa KK, Gordon JG. Frequency of a quartz microbalance in contact with liquid. *Analytical Chemistry.* 1985;57(8):1770-1771.

23. Curie J CP. An oscillating quartz crystal mass detector. *Rendu.* 1880;91:294-297.

24. D. S. Ballantine. *Acoustic wave sensors : theory, design, and physico-chemical applications*. San Diego: Academic Press; 1997.

25. Newell WE. Face-mounted piezoelectric resonators. *Proceedings of the IEEE.* 1965;53:575-581.

26. Shons A, Dorman F, Najarian J. An immunospecific microbalance. *Journal of Biomedical Materials Research.* 1972;6(6):565-570.

27. Sang-Hun Lee DDS, John Cairney, and William D. Hunt. Rapid Detection of Bacterial Spores Using a Quartz Crystal Microbalance (QCM) Immunoassay. *IEEE SENSORS JOURNAL.* 2005;5(4):737-743.

28. William Hunt DS, and Sang-Hun Lee. Time-Dependent Signatures of Acoustic Wave Biosensors. *Proceedings of the IEEE.* 2003;91(6):890-902.

29. Hunt W. Clues from Digital Radio Regarding Biomolecular Recognition. Paper presented at: Cancer Biology Lecture2009.

30. Ludwig JA, Weinstein JN. Biomarkers in Cancer Staging, Prognosis and Treatment Selection. *Nat Rev Cancer.* 2005;5(11):845-856.

31. Engvall E PP. Enzyme-linked immunosorbent assay (ELISA). Quantitative assay of immunoglobulin G. *Immunochemistry.* 1971;8(9):871-874.

32. Bunte G, Hürttlen J, Pontius H, Hartlieb K, Krause H. Gas phase detection of explosives such as 2,4,6-trinitrotoluene by molecularly imprinted polymers. *Analytica Chimica Acta.* 2007;591(1):49-56.

33. Sang-Hun Lee Stubbs DDC, J. Hunt, W.D. Rapid detection of bacterial spores using a quartz crystal microbalance (QCM) immunoassay. *Sensors Journal, IEEE.* 2005;5(4).

34. Mello LD, Kubota LT. Review of the use of biosensors as analytical tools in the food and drink industries. *Food Chemistry.* 2002;77(2):237-256.

35. Uttenthaler E, Kößlinger C, Drost S. Quartz crystal biosensor for detection of the African Swine Fever disease. *Analytica Chimica Acta.* 1998;362(1):91-100.

36. Braunhut SJ MD, Vorotnikova E, Zhou T, Marx KA. Detection of apoptosis and drug resistance of human breast cancer cells to taxane treatments using quartz crystal microbalance biosensor technology. *ASSAY and Drug Development Technologies.* 2005;3(1):77-88.

37. Christopher Corso DS, Sang-Hun Lee, Michael Goggins, Ralph Hruban, William Hunt. Real-time detection of mesothelin in pancreatic cancer cell line supernatant using an acoustic wave immunosensor. *Cancer Detection and Prevention.* 2006;30:180-187.

38. Muratsugu M, Ohta F, Miya Y, et al. Quartz crystal microbalance for the detection of microgram quantities of human serum albumin: relationship between the frequency change and the mass of protein adsorbed. *Analytical Chemistry.* 1993;65(20):2933-2937.

39. Chou S-F, Hsu W-L, Hwang J-M, Chen C-Y. Development of an immunosensor for human ferritin, a nonspecific tumor marker, based on a quartz crystal microbalance. *Analytica Chimica Acta.* 2002;453(2):181-189.

40. Johannsmann D. Studies of Viscoelasticity with the QCM. In: Steinem C, Janshoff A, eds. *Piezoelectric Sensors.* Vol 5: Springer Berlin Heidelberg; 2007:49-109.

41. Bain CD, Whitesides GM. Molecular-Level Control over Surface Order in Self-Assembled Monolayer Films of Thiols on Gold. *Science.* 1988;240(4848):62-63.

42. Prime KL, Whitesides GM. Self-Assembled Organic Monolayers: Model Systems for Studying Adsorption of Proteins at Surfaces. *Science.* 1991;252(5009):1164-1167.

43. POLJAK BCBARJ. Structural features of the reactions between antibodies and protein antigens. *The FASEB Journal.* 1995;9:9-16.

44. Voinova MV. On Mass Loading and Dissipation Measured with Acoustic Wave Sensors: A Review. *Journal of Sensors.* 2009;2009.

45. Wright AK, Thompson MR. Hydrodynamic structure of bovine serum albumin determined by transient electric birefringence. *Biophysical journal.* 1975;15(2):137-141.

VITA

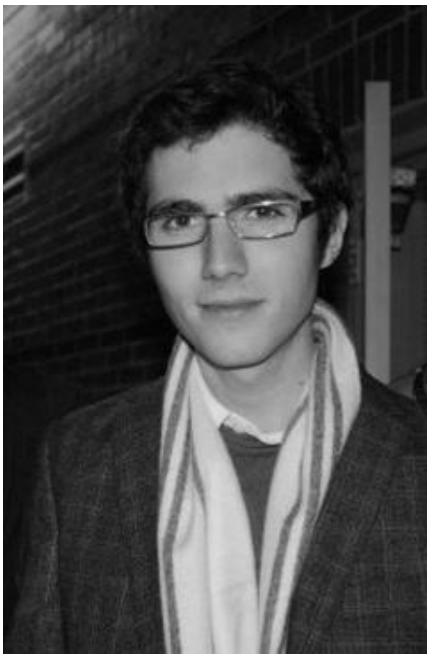

Christopher Giardina is an Honors Program student at the Georgia Institute of Technology currently completing his B.S. in Biomedical Engineering with a minor in Biology and focuses on pre-medicine and translational research. In addition to prostate cancer detection, he also performed research to investigate the cellular mechanisms of soy and tomato isoflavones on prostate cancer prevention. Prior to cancer research, he investigated in a neuroengineering laboratory designing polymers to induce and direct neuron growth. He is the recipient of the Georgia Cancer Coalition's Carpenter Fellowship, has prepared 3 publications, and has twice been awarded the Georgia Tech Presidential Undergraduate Research Awards scholarship. He is currently patenting a surgical device to assist in cataract surgery. He will enroll in an MD/PhD program in Fall of 2011.